PHILOSOPHICAL TRANSACTIONS OF THE ROYAL SOCIETY A MATHEMATICAL, PHYSICAL & ENGINEERING SCIENCES

Spectroscopy of the Hydrogen Molecular Ion at its Dissociation Limit [and Discussion]

A. Carrington, I. R. McNab, Christine A. Montgomerie, C. Whitham and W. H. Wing

Phil. Trans. R. Soc. Lond. A 1988 **324**, 275-287
doi: 10.1098/rsta.1988.0017

Phil. Trans. R. Soc. Lond. A **324**, 275–287 (1988)
Printed in Great Britain

Spectroscopy of the hydrogen molecular ion at its dissociation limit

By A. Carrington†, F.R.S., I. R. McNab and Christine A. Montgomerie
Physical Chemistry Laboratory, University of Oxford, South Parks Road, Oxford OX1 3QZ, U.K.

Previous theoretical and experimental work on the ion H_2^+ and its deuterium isotopes HD^+ and D_2^+ is briefly reviewed. Spectroscopic studies of the vibration–rotation levels are discussed, and recent work on the infrared photodissociation of the high-lying vibrational levels is described. Earlier work that made use of ion-beam techniques to study the vibration–rotation levels of HD^+ is reviewed, and compared with the most recent theoretical predictions.

The nuclear-hyperfine and spin–rotation structure of HD^+ is described, and recent observations of the vibration–rotation satellite lines that will yield absolute values of the deuterium hyperfine constants are presented. We conclude by describing our attempts to observe radiofrequency–infrared double-resonance spectra.

1. Introduction

The hydrogen molecular ion occupies a central position in the development of molecular quantum mechanics. A detailed review (Carrington & Kennedy 1984) has been presented elsewhere, and a short summary of the underlying theory here will suffice to establish the context of our current work. The hydrogen molecular ion (and its isotopic variants) contains two nuclei and one electron, and is therefore the molecular example of the quantum-mechanical three-body problem. Because this problem cannot be solved exactly, theoretical studies have been directed towards appropriate approximate treatments that yield values of the energy levels and other molecular constants. Electron–electron interactions are, of course, not present in this simple molecule; consequently the focus of attention is on the nuclear and electronic motions, and their mutual interactions. Calculations may be classified under three main headings. Born–Oppenheimer calculations attempt to solve the problem of the electron moving in the electrostatic field of two fixed nuclei. The Schrödinger equation for this system may be separated into three one-dimensional differential equations (Alexandrow 1926) and exact numerical solutions obtained (Burrau 1927). Analytical solutions with series expansions were developed (Hylleraas 1931; Jaffé 1934) and have been the basis of much subsequent work.

Inclusion of cross terms between the nuclear and electronic kinetic-energy operators that are diagonal in the ground electronic state constitutes the adiabatic approximation and the first complete calculations of all bound vibration–rotation levels of H_2^+, HD^+ and D_2^+ were provided by Hunter *et al.* (1974). Figure 1 shows the highest-lying vibrational levels of the three isotopes in their ground electronic state ($^2\Sigma_g^+$); the first excited electronic state ($^2\Sigma_u^+$), which also correlates with the lowest dissociation limits, is repulsive at all internuclear distances (except for a van der Waals minimum), a fact that is crucial to our experimental studies. Non-adiabatic corrections to these energy levels involve the coupling of different electronic states by the nuclear kinetic energy. This problem was first tackled by Bishop & Cheung (1977), and calculations for all bound vibrational levels have been presented by Wolniewicz & Poll (1978, 1986). Radiative

† Present address: Department of Chemistry, University of Southampton, Southampton SO9 5NH, U.K.

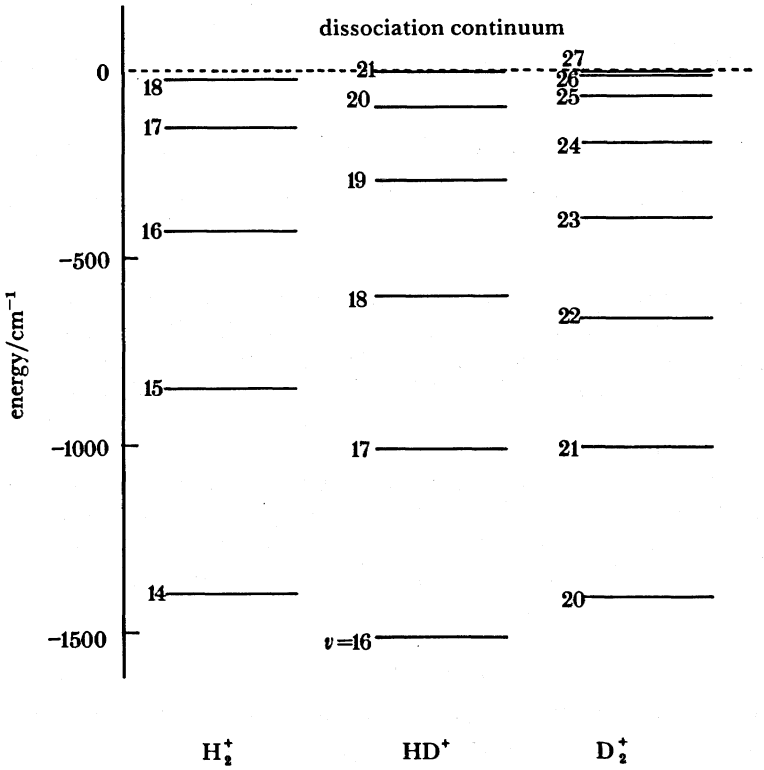

FIGURE 1. Highest-energy vibrational levels for H_2^+, HD^+ and D_2^+ in their ground electronic states, based upon the calculations of Hunter *et al.* (1974).

and relativistic corrections have also been included in the calculations of Wolniewicz & Poll.

Laboratory spectroscopic studies of H_2^+ and its isotopes are difficult, particularly because the only bound excited electronic states predicted by theory lie at energies more than 11 eV above the ground state; conventional electronic spectroscopy is therefore not possible. A notable early achievement was the measurement of the radiofrequency spectra of H_2^+ in vibrational levels $v = 4$–8 by an ingenious method that involved quadrupole trapping of the ion and spatial alignment produced by photodissociation with polarized white light (Dehmelt & Jefferts 1962; Jefferts 1968, 1969). The principles underlying this method will be discussed later. Apart from this exceptional study, however, most of our earlier knowledge of the vibrational levels of H_2^+ and its isotopes came from photoelectron studies (Åsbrink 1970; Pollard *et al.* 1982), photoionization studies (Chupka & Berkowitz 1969; Peatman 1976) and Rydberg spectra (Takezawa 1970*a*, *b*; Herzberg & Jungen 1972). The first measurement of a vibration–rotation spectrum of HD^+ (and indeed, of any molecular ion) was described in 1976 by Wing *et al.* They employed Doppler tuning of a fast HD^+ ion beam to bring vibration–rotation transitions into resonance with a carbon monoxide infrared laser frequency; excitation was detected through the resulting changes in the charge-exchange attenuation of the HD^+ beam, produced by added neutral gases. Spectra involving the lowest vibrational levels ($v = 0$–3) were studied, and transition frequencies accurate to 0.001 cm^{-1} determined.

2. Infrared photodissociation

An important feature of ion-beam studies is that electron impact ionization of H_2 and its isotopes results in population of all the bound vibrational levels of the ground state up to the dissociation limit; these populations are preserved in the collision-free environment of an ion beam system. Because the first excited state is repulsive, ions in the highest-energy vibrational levels can be photodissociated with infrared radiation. This point was appreciated by Fournier *et al.* (1979) who calculated cross sections for photodissociation in the frequency range covered by the carbon dioxide laser (900–1100 cm^{-1}). The photodissociation is central to our spectroscopic studies of HD^+, and we have recently carried out a crossed-beam study in which the relative photodissociation cross sections for the highest-energy vibrational levels of H_2^+, HD^+ and D_2^+ are essentially determined. The apparatus, which is also used for the spectroscopic studies described in §3, has been described extensively elsewhere (Carrington & Buttenshaw 1981; Carrington & Kennedy 1984) and is illustrated schematically in figure 2. The ions are formed by electron-impact ionization, with electron energies up to 100 eV, and are accelerated to potentials up to a maximum of 10 kV. Mass analysis of the ion beam is achieved with a 55° magnetic sector, and the desired ion beam is then brought into coincidence with a focused carbon dioxide infrared laser beam, aligned either collinear with, or perpendicular to, the ion beam. Photofragment ions are separated from the parent ions with an 81.5° electrostatic analyser (ESA) and detected with an off-axis electron multiplier.

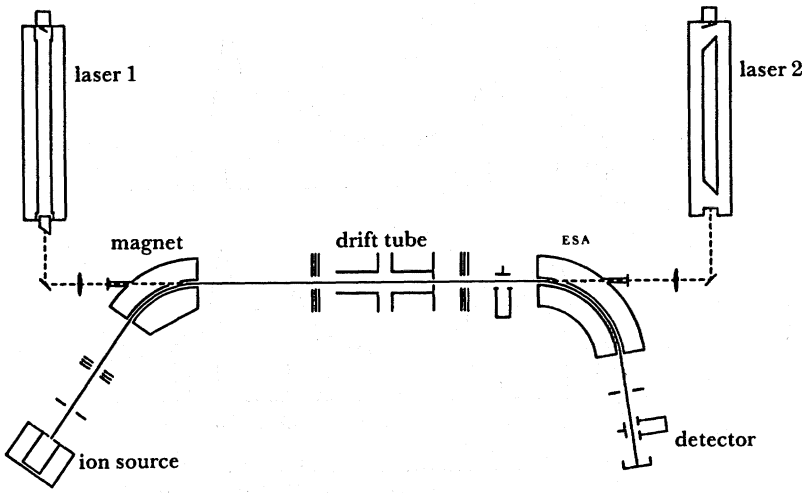

Figure 2. Schematic diagram of the tandem mass spectrometer (Vacuum Generators ZAB 1F instrument with modifications).

The ion beam comes to a focal point that is at the centre of a cylindrical drift tube situated between the magnetic and electric sectors. This region of the apparatus is very important for the spectroscopic studies described in the next section, and will be discussed in more detail therein.

The energy resolution of the ESA is sufficiently high for the laboratory kinetic energy of the photofragment ions to be determined; a suitable transformation to the centre of mass can then be performed. Because the electronic transition in H_2^+ leading to photodissociation is polarized

along the internuclear axis, crossed-beam irradiation, with the electric vector parallel to the ion beam, leads to preferential production of protons in the forward and backward directions of the parent ion beam. The irradiation point is close to the ion-beam focal point at the centre of the drift tube, and the photofragment kinetic-energy spectra are obtained by scanning the ESA voltage. Slits before and after the ESA are adjusted to optimize resolution, at the cost of fragment ion-beam intensity. Our best results for H_2^+, which were obtained by chopping the laser beam and detecting the AC photofragment current with a lock-in amplifier, are shown in figure 3;

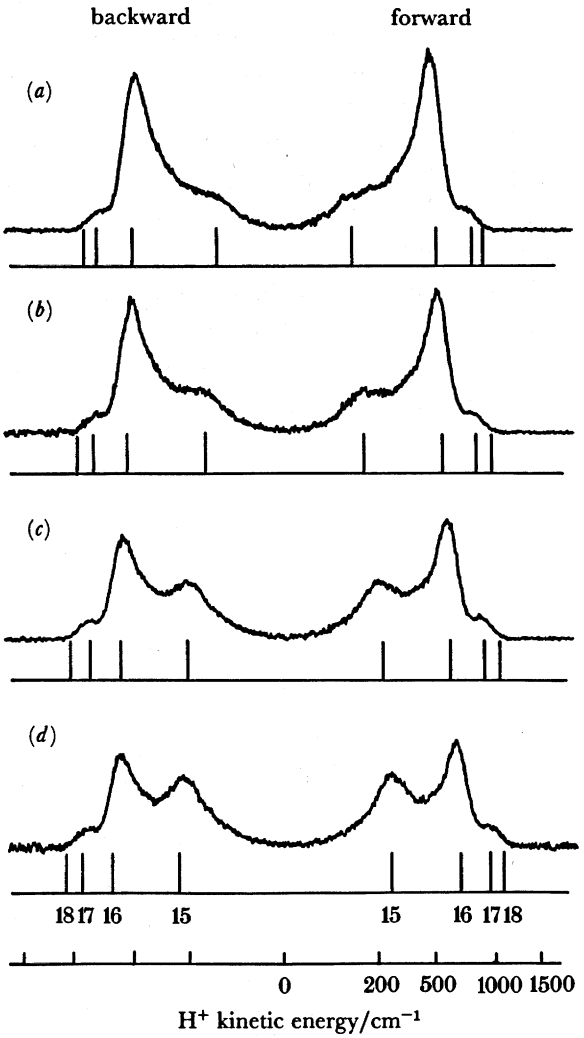

FIGURE 3. Photofragment H^+ kinetic-energy spectra obtained for H_2^+ at four different laser frequencies: (*a*) 938.69; (*b*) 979.70; (*c*) 1041.28; (*d*) 1082.29 cm^{-1}.

spectra at four different laser wavelengths with an average laser power of 30 W cw are shown. Vibrational structure is resolved, and it is clear that the photodissociation cross section is largest for $v = 16$; it should be noted, however, that the spectra shown in figure 3 reflect both the photodissociation cross sections, the vibrational-level populations, and instrumental factors that give an intensity dependence roughly proportional to the inverse of the centre-of-mass

kinetic-energy release. Structure due to ions in the highest vibrational level, $v = 18$, is not resolved and the cross section at these frequencies is probably small, but crucially not zero. Similar studies of HD^+ and D_2^+ show only one peak for HD^+ (from $v = 18$) at all four laser frequencies, but with D_2^+ peaks due to ions in $v = 22$, 23 and 24 are resolved, particularly at the lowest-used laser frequency of 938.69 cm^{-1}.

3. Two-photon vibration–rotation spectra of HD^+

Figure 4 shows the potential curves for the ground and first excited electronic states of HD^+, and the highest vibrational levels of the ground state. As we have already noted, ions in $v \geqslant 18$ will be photodissociated by infrared radiation from a carbon dioxide laser (900–1100 cm^{-1}) but those of low rotational quantum number in $v \leqslant 17$ will not. Consequently vibration–rotation transitions, such as those belonging to the 17–20 band shown in figure 4, can be detected through the resulting increase in the number of photoproduct H^+ or D^+ ions. Most of our previous work has been carried out with the apparatus shown in figure 2. The laser beam is aligned to be collinear with the ion beam, either parallel or antiparallel. Coarse frequency scanning is achieved by selecting an appropriate carbon dioxide laser line, and fine tuning results from scanning the Doppler shift by changing the ion-beam potential.

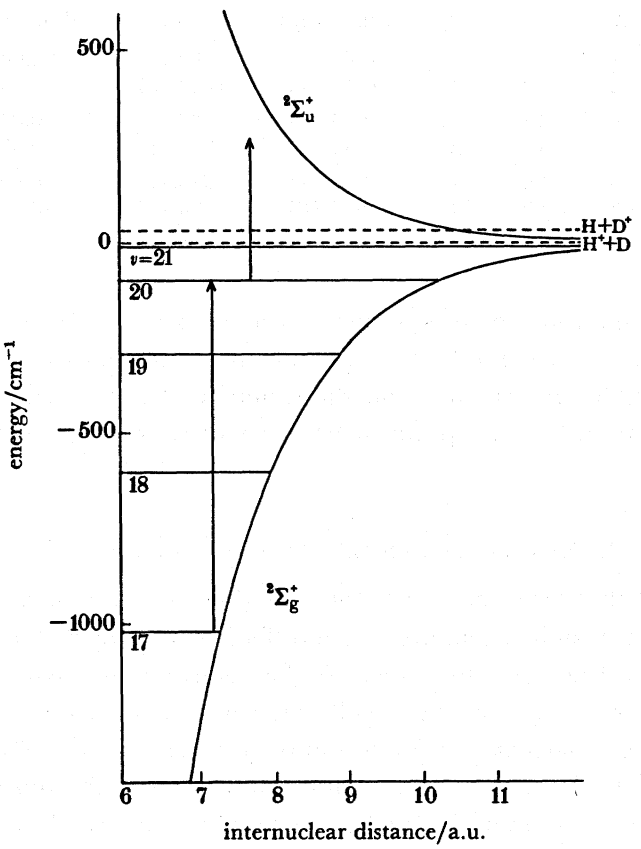

Figure 4. Potential-energy curves for the ground and first excited electronic states of HD^+, in the vicinity of the dissociation limits. (1 a.u. (length) = 1 Bohr $\approx 0.529 \times 10^{-10}$ m.)

For an ion as light as HD^+, beam potentials from 1 to 10 kV, with positive or negative Doppler shifts, provide complete frequency tuning from one laser line to the next.

The ESA is used to separate the fragment ions (we usually choose to monitor D^+) from the parent ions. We apply an oscillating voltage to the drift tube shown in figure 2; this produces velocity modulation of the ion beam and hence, through the Doppler effect, frequency modulation. Consequently, vibration–rotation transitions are located by detecting the AC photofragment current from the electron multiplier with a lock-in amplifier.

The sensitivity of the method is high, and transitions in the $v = 16$–18 band an be detected with signal:noise ratios of approximately 1000:1 (Carrington & Buttenshaw 1981). It proved to be advantageous to use two lasers, one operating at high powers (typically 20 W CW) to maximize the photofragment intensity, and the other at lower powers (1–2 W) to drive the vibration–rotation transitions. Measurements of rotational components of the 16–18, 14–17, 15–17 and 17–20 bands have been described. In many cases we were able to make more than one independent measurement of a particular vibration–rotation transition by using different laser lines at different ion-beam potentials, aligned parallel or antiparallel. The resulting cancellation of systematic errors means that vibration–rotation frequencies were measured with an accuracy better than 0.001 cm^{-1}. This provides a severe test of the accuracy of *ab initio*

TABLE 1. VIBRATION–ROTATION TRANSITIONS (RECIPROCAL CENTIMETRES) IN HD^+

v''	N''	v'	N'	experiment	theory	difference
0	1	1	0	1869.134	1869.131	+0.003
2	2	3	1	1642.108	1642.107	+0.001
16	0	18	1	926.490	926.494	−0.004
16	2	18	3	933.213	933.217	−0.004
17	0	20	1	918.102	918.111	−0.009
17	3	20	4	885.749	885.767	−0.018

calculations, which have improved progressively over the past fifteen years. Table 1 presents a brief selection of the experimental data and the most recent theoretical calculations of Wolniewicz & Poll (1986). As can be seen, the difference between experiment and theory increases as the dissociation limit is approached; nevertheless the agreement is impressive.

4. NUCLEAR HYPERFINE INTERACTIONS

A fascinating feature that arises in the case of HD^+ (but not with H_2^+ or D_2^+) is the presence of two dissociation limits, as shown in figure 4, that differ in energy by 29.8 cm^{-1}. This difference arises because of the difference in reduced mass of the electron in the hydrogen and deuterium atoms. The question arises, therefore, as to whether the electron distribution in HD^+ is sensitive to this energy difference, particularly for vibration–rotation levels approaching the lower dissociation limit, $H^+ + D$. From an experimental point of view, the route to answering this question lies through observation of the nuclear hyperfine structure of the vibration–rotation transitions.

The proton and deuteron have nuclear spins of $\frac{1}{2}$ and 1 respectively, and there will be

PHILOSOPHICAL TRANSACTIONS OF THE ROYAL SOCIETY A MATHEMATICAL, PHYSICAL & ENGINEERING SCIENCES

magnetic hyperfine interactions with the electron spin S of $\frac{1}{2}$. In addition, one expects a magnetic interaction between the magnetic moments caused by electron spin and nuclear rotation. The expected relative magnitudes of these interactions suggests that the most appropriate scheme for coupling the various angular momenta is the following:

$$\begin{aligned} S+I_{\mathrm{H}} &= G_1 \quad G_1 = \quad 1 \quad ;0, \\ G_1+I_{\mathrm{D}} &= G_2 \quad G_2 = 2, 1, 0; 1, \\ G_2+N &= F. \end{aligned}$$

Possible values of the quantum numbers G_1 and G_2 are shown. The most significant hyperfine constants, with approximate estimates of their values for the highest-lying vibrational levels, are as follows:

b_{H}, the proton Fermi contact interaction (less than or equal to 720 MHz);
b_{D}, the deuteron Fermi contact interaction (more than or equal to 110 MHz);
t_{H}, the axial component of the proton dipolar interaction (less than or equal to 12 MHz);
t_{D}, the axial component of the deuteron dipolar interaction (less than or equal to 2 MHz);
γ, the spin–rotation interaction (less than or equal to 10 MHz).

Many other interactions are also present, but their magnitudes will be much smaller. Carrington & Kennedy (1985) have given explicit expressions for all the relevant matrix elements of the hyperfine interactions in the above basis, and have also made theoretical calculations of the values of different hyperfine constants. The hyperfine level structure for the vibration–rotation transition 16, 1–18, 2 is shown in figure 5. For each vibration–rotation level there is a large doublet splitting ($G_1 = 1$ and 0) arising from the proton Fermi contact interaction, a triplet splitting ($G_2 = 2, 1, 0$) of the $G_1 = 1$ level, from the deuteron Fermi contact term, and much smaller splittings of each G_1, G_2 level caused by the spin–rotation interaction.

It is clear from figure 5 that many different transitions are possible, and we shall discuss all of these in due course. However, the allowed electric-dipole vibration–rotation transitions must satisfy the selection rules

$$\Delta N = \pm 1, \quad \Delta G_1 = 0, \quad \Delta G_2 = 0, \quad \Delta F = 0, \pm 1.$$

Leaving aside the small spin–rotation splittings, we see that there are four transitions that satisfy these selection rules. Any observed hyperfine splitting of the allowed vibration–rotation transitions will depend only on the differences in hyperfine splitting for the upper and lower states.

At high laser powers, the observed vibration–rotation resonances consist of a single line of width 30–40 MHz, but at lower laser powers it was soon found that every transition exhibits a characteristic doublet splitting (typically 10–20 MHz). The two lines arise from levels with $G_1 = 0$ or 1 and the splitting shows that the proton hyperfine splitting in the upper level is the smaller.

For vibration–rotation levels approaching the dissociation limit $H^+ + D$, one might expect the proton splitting in HD^+ to decrease, with a corresponding increase in the deuteron splitting. The deuteron magnetogyric ratio is nearly seven times smaller than that of the proton, so that changes in the deuteron hyperfine splitting are much smaller and therefore more difficult to observe. Observation of levels with $v = 20$ or 21 would provide a critical test of these expectations and they were indeed confirmed by Carrington & Kennedy (1985) through

PHILOSOPHICAL TRANSACTIONS OF THE ROYAL SOCIETY A MATHEMATICAL, PHYSICAL & ENGINEERING SCIENCES

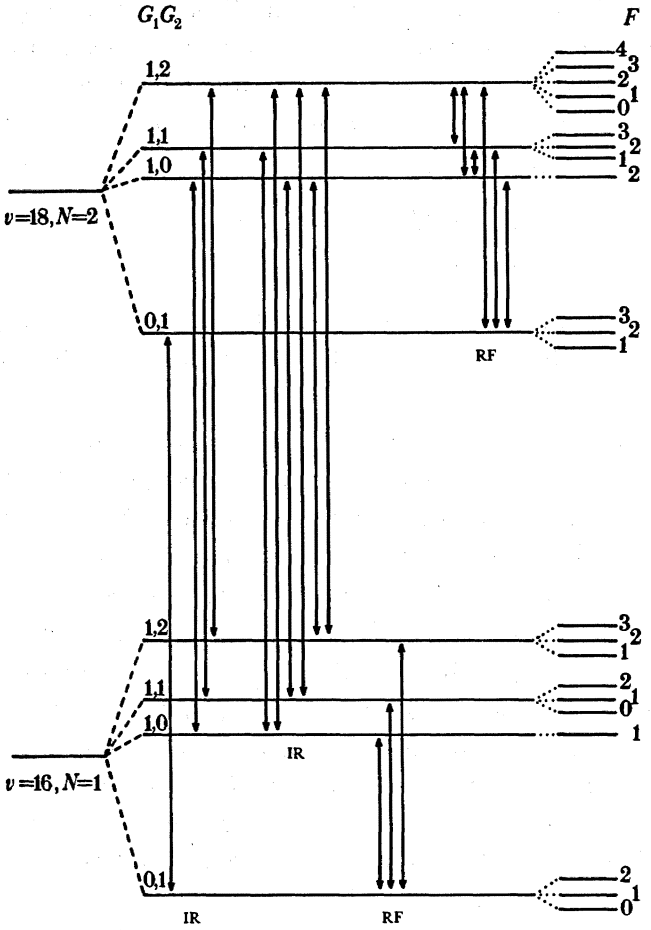

FIGURE 5. Nuclear-hyperfine and spin–rotation structure of two vibration–rotation levels of HD^+. The electric-dipole allowed vibration–rotation transitions are shown on the left, the forbidden transitions are shown in the centre, and possible radiofrequency transitions are shown to the right.

measurements of the 17–20 band. The observed proton hyperfine splittings ranged from 80 to 125 MHz, and additional splitting due to the increased deuteron interaction was observed, proving unambiguously that the electron distribution in HD^+ does indeed become asymmetric as the $H^+ + D$ dissociation limit is approached. The highest level to be observed was $v = 20$, $N = 4$, which lies 47 cm^{-1} below the dissociation limit. Theoretical calculations that took into account the non-adiabatic coupling of the ground and first excited states provided a satisfactory interpretation of the observed spectra.

It is unfortunate that the allowed electric-dipole transitions are necessarily diagonal in G_1 and G_2 and hence cannot usually yield absolute values of the nuclear hyperfine constants. Transitions that formally follow selection rules $\Delta G_1 = \pm 1$ or $\Delta G_2 = \pm 1$ acquire electric-dipole intensity only through the spin–rotation and nuclear-dipolar interactions, which mix states differing in G_1 and G_2. The mixing is predicted to be very small, because the necessary interactions are small, so that $\Delta G_2 \neq 0$ transitions such as those shown in figure 5 are predicted to be three orders of magnitude weaker than the fully allowed transitions. Weak satellites were reported by Carrington & Buttenshaw (1981) but they were not reproducible and were not studied in detail.

We have recently built a new ion-beam machine that has resulted in increased sensitivity, so that the $\Delta G_2 \neq 0$ satellites are clearly and reproducibly observable. The new machine is shown schematically in figure 6, and is very similar to an earlier instrument (Carrington *et al.* 1979). It consists of two 90° magnetic sectors, with focusing lenses between them, and an ion-beam path between the sectors of only 50 cm. Ironically, this machine was actually built for

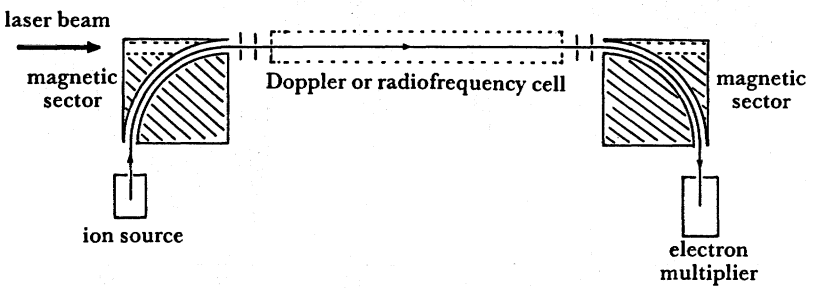

FIGURE 6. Tandem ion-beam system employing two 90° magnetic sectors (see text).

the double-resonance experiments described in the next section. It is much smaller than the machine described in figure 2; consequently tighter focusing of the ion and laser beams is possible, and this probably accounts for the increased sensitivity.

Figure 7 shows a very recent recording of the 16, 1–18, 2 transition in which the $\Delta G_2 = \pm 1$ satellites are clearly observable. Guided by the calculations of Carrington & Kennedy (1985) we are able to assign these satellites, as shown. Similar satellite structure has been observed for the 16, 2–18, 3 transition and we expect to be able to determine absolute values of at least the deuteron Fermi contact constants for the upper and lower states. The enhanced sensitivity has also enabled us to improve the resolution of the strongly allowed electric–dipole transitions, and figure 8 shows the 16, 1–18, 2 transition, now split into four components, rather than just two as described recently. We can assign the values of G_1 with some confidence; it is tempting

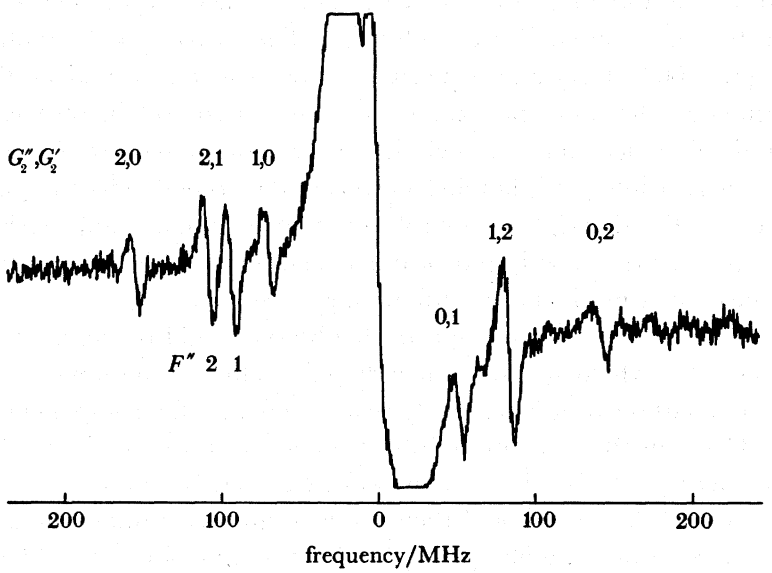

FIGURE 7. The 16, 1–18, 2 vibration–rotation transition (932.2237 cm^{-1}) in HD^+, showing the $\Delta G_2 = \pm 1$ satellites.

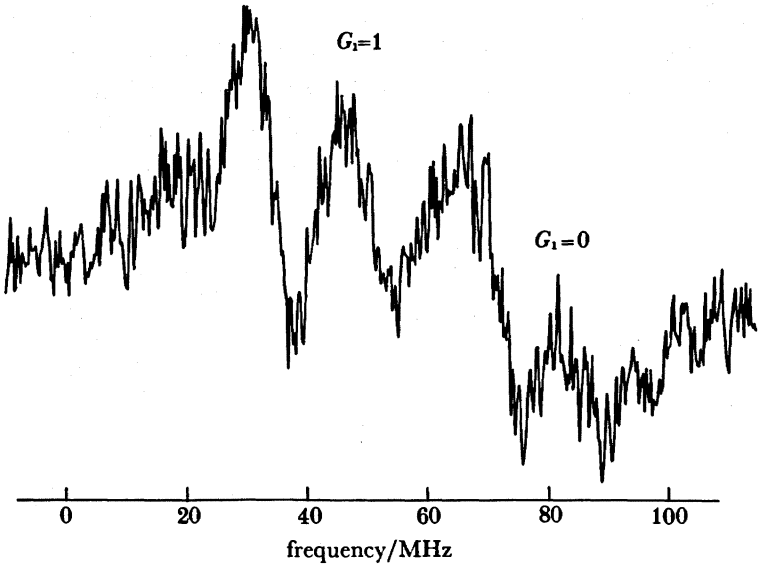

FIGURE 8. The resolution of the electric-dipole allowed components of the 16, 1–18, 2 vibration–rotation transition (932.2237 cm^{-1}) in HD^+, plotted on a relative frequency scale in MHz.

to assign the three $G_1 = 1$ peaks to $G_2 = 2, 1, 0$, but this may be an over-simplification. There is every reason to suppose that we will be able to observe $\Delta G_2 = \pm 1$ satellite transitions for other vibrational-band systems.

Unfortunately, the $\Delta G_1 = \pm 1$ satellite transitions, which would yield the proton hyperfine constants, are predicted to be very much weaker than the $\Delta G_2 = \pm 1$ transitions because the hyperfine states are much more widely separated and therefore less mixed by the coupling terms. We have not yet succeeded in observing such satellites, but the searches will continue.

5. RADIOFREQUENCY–INFRARED DOUBLE-RESONANCE EXPERIMENTS

It would be most desirable to be able to measure the nuclear-hyperfine transitions directly; examples of these transitions are indicated in figure 5. They occur in the radiofrequency region of the spectrum (10–1000 MHz) and a possible route to success would be through double-resonance experiments. (Because the experiments on $v = 16$ still involve excitation to the repulsive state and subsequent photodissociation, they actually require the absorption of one radiofrequency and two infrared photons; however, the second infrared photon excites to a continuum state so the description 'double resonance' is more appropriate than 'triple resonance'.) We give a brief description of our experiments, although we have not, at the time of writing, succeeded in observing radiofrequency spectra.

Potentially the easiest radiofrequency spectra to observe would be those involving the lower vibration–rotation states, which are not excited directly to the continuum by the infrared laser. As we have already mentioned, it is relatively easy to separate the components corresponding to $G_1 = 1$ and 0. Consequently we aim to adjust the ion-beam potential so that one of these transition groups (say $G_1 = 0$) is driven by the infrared laser. Radiofrequency transitions that obey the selection rule $\Delta G_1 = \pm 1$ would then result in increased photofragmention.

A second, and more subtle, radiofrequency study is possible for states (like $v = 18$, $N = 2$,

PHILOSOPHICAL TRANSACTIONS OF THE ROYAL SOCIETY A MATHEMATICAL, PHYSICAL & ENGINEERING SCIENCES

shown in figure 5) that are excited directly to the repulsive state by the infrared laser. The principles involved are exactly those described and exploited by Dehmelt & Jefferts (1962) in their study of the lower vibrational levels of H_2^+. Photodissociation of 18, 2, for example, obeys the selection $\Delta M_F = 0$, where the quantization axis is defined by the direction of the electric vector of the infrared laser. Consequently states of different M_F value photodissociate at different rates, so that the remaining undissociated ions exhibit a degree of spatial alignment. The development of spatial alignment is reflected in the cross section for photodissociation. Pumping of different F levels by a radiofrequency magnetic field will change the degree of alignment, and for $\Delta M_F = \pm 1$ transitions remove it altogether, so that the photodissociation rate will increase. We therefore monitor the production of photofragment ions as a function of the radiofrequency. It is not necessary to drive simultaneously an allowed vibration–rotation transition. One of the most attractive features of this experiment is that, because magnetic dipole transitions are involved, we are not restricted to the heteronuclear species HD^+.

We have attempted many different methods of coupling radiofrequency power to the ion beam, and our present method is based on that described by Rosner *et al.* (1978) in their studies of the Xe^+ ion. It is shown schematically in figure 9. The radiofrequency cell consists of a

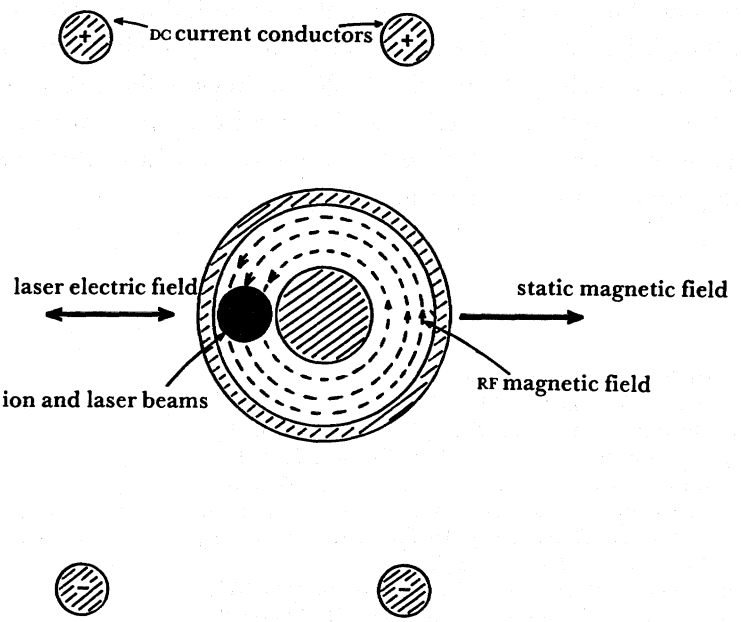

FIGURE 9. Relative orientations of the ion and laser beams, radiofrequency coaxial cell, and four-pole current conductors employed in double-resonance experiments.

coaxial arrangement of inner and outer copper tubes, with the ion and laser beams transmitted between the conductors as shown. The present device is 36 cm in length, and radiofrequency power is coupled in and out by modified coaxial cable connectors. Care is taken to maintain a 50 Ω impedance throughout the frequency range, and we are able to couple in at least 10 W through the range 10–1000 MHz. As shown in figure 9 the radiofrequency magnetic field is mainly perpendicular to the ion-beam axis and to the electric vector of the laser beam. In addition, the coaxial cell resides inside a four-pole structure supplied with DC current to produce a static magnetic field (if required) that is parallel to the laser electric vector. We amplitude-

or frequency-modulate the radiofrequency power, and detect the photofragment current at the modulation frequency.

We have adopted the present method only recently, and have not yet succeeded in detecting radiofrequency resonances. The radiofrequency magnetic field at the ion beam is calculated to be approximately 0.1 G†, and although we believe this should be sufficient, it may be marginal. Resonant high-Q devices would, of course, give much higher radiofrequency fields, but frequency tuning then becomes difficult.

As we have mentioned, one of the most attractive features of the radiofrequency experiment that depends upon spatial alignment is its potential application to the homonuclear species H_2^+ and D_2^+. Our infrared studies have necessarily been restricted to the heteronuclear species, HD^+, which possesses the necessary electric-dipole moment. It may well be the most interesting of the three species because of the existence of the two close-lying dissociation limits, and there is still much to be revealed about the details of this system. Even though the large asymmetry observed for HD^+ is not expected for H_2^+ and D_2^+, it is nevertheless possible that they will also exhibit surprising nuclear-hyperfine effects at their dissociation limits.

We are most grateful to Mr Roger Bowler for his superb workmanship in the extensive machining necessary for this work. We would like to thank Professor S. D. Rosner and Professor R. A. Holt of the University of Western Ontario for their advice concerning the design of the coaxial radiofrequency cell. A.C. thanks the Royal Society for a Research Professorship, and I.R.M. and C.A.M. thank the SERC and The British Petroleum Company plc respectively for post-graduate research studentships. We are also grateful to the SERC for their financial support in the purchase and construction of equipment.

References

Alexandrow, W. 1926 *Ann. Phys.* **81**, 603–614.
Åsbrink, L. 1970 *Chem. Phys. Lett.* **7**, 549–552.
Bishop, D. M. & Cheung, L. M. 1977 *Phys. Rev.* A **16**, 640–645.
Burrau, Ø. 1927 *K. danske Vidensk. Selsk. Math. Fys. Meddr.* **7**, 14.
Carrington, A. & Buttenshaw, J. 1981 *Molec. Phys.* **44**, 267–285.
Carrington, A., Buttenshaw, J. & Roberts, P. G. 1979 *Molec. Phys.* **38**, 1711–1715.
Carrington, A. & Kennedy, R. A. 1984 In *Gas phase ion chemistry*, vol. 3 (*Ions and light*) (ed. M. T. Bowers), pp. 393–442. London: Academic Press, Inc.
Carrington, A. & Kennedy, R. A. 1985 *Molec. Phys.* **56**, 935–975.
Chupka, W. A. & Berkowitz, J. 1969 *J. chem. Phys.* **51**, 4244–4268.
Dehmelt, H. G. & Jefferts, K. B. 1962 *Phys. Rev.* **125**, 1318–1322.
Fournier, P., Lassier-Govers, B. & Comtet, G. 1979 In *Laser-induced processes in molecules* (ed. K. L. Kompa & S. D. Smith), pp. 247–251. Berlin & New York: Springer Verlag.
Herzberg, G. & Jungen, Ch. 1972 *J. molec. Spectrosc.* **41**, 425–486.
Hunter, G., Yau, A. W. & Pritchard, H. O. 1974 *Atom. Data Nucl. Data Tables* **14**, 11–20.
Hylleraas, E. A. 1931 *Z. Phys.* **71**, 739–763.
Jaffé, G. 1934 *Z. Phys.* **87**, 535–544.
Jefferts, K. B. 1968 *Phys. Rev. Lett.* **20**, 39–41.
Jefferts, K. B. 1969 *Phys. Rev. Lett.* **23**, 1476–1478.
Peatman, W. B. 1976 *J. chem. Phys.* **64**, 4093–4099.
Pollard, J. E., Trevor, D. J., Reutt, J. E., Lee, Y. T. & Shirley, D. A. 1982 *J. chem. Phys.* **77**, 34–46.
Rosner, S. D., Gaily, T. D. & Holt, R. A. 1978 *Phys. Rev. Lett.* **40**, 851–854.
Takezawa, S. 1970*a* *J. chem. Phys.* **52**, 2575–2590.

† 1 G = 10^{-4} T.

Takezawa, S. 1970*b* *J. chem. Phys.* **52**, 5793–5799.
Wing, W. H., Ruff, G. A., Lamb, W. E. & Spezeski, J. J. 1976 *Phys. Rev. Lett.* **36**, 1488–1491.
Wolniewicz, L. & Poll, J. D. 1978 *J. molec. Spectrosc.* **72**, 264–274.
Wolniewicz, L. & Poll, J. D. 1986 *Molec. Phys.* **59**, 953–964.

Discussion

C. WHITHAM (*Department of Chemistry, University of Nottingham, Nottingham, U.K.*). The first excited state of HD^+ is calculated to possess a shallow ion-induced dipole well. Does Professor Carrington think that there is a possibility of observing levels supported by this well?

A. CARRINGTON, F.R.S. The first excited electronic states of H_2^+, HD^+ and D_2^+ each possess long-range minima arising from the charge-induced dipole interaction; these should perhaps be called Langevin minima. They certainly support vibration–rotation levels, and electronic transitions from the ground states are allowed. The only problem is to devise a scheme for detecting such transitions! We are following various possibilities in laboratory work at the present time.

W. H. WING (*Department of Physics, University of Arizona, Tucson, U.S.A.*). I should like to mention two effects in addition to accurate non-adiabatic energies that must be included to gain good agreement between theory and experiment for HD^+. The first of these is the relativistic mass increase of the electron that arises on account of its kinetic energy. The second is the shift in the electron's energy that stems from the zitterbewegung in the electron's motion, caused by quantum-electrodynamic zero-point radiation field fluctuations. This 'jiggling motion' introduces an effective term in the electron hamiltonian that is proportional to the potential curvature near the nuclei and corresponds to the Lamb Shift in atomic energies. When these electronic eigenenergy shifts are averaged over the nuclear motion, they cause spectroscopically observable shifts of about 10 and 5 p.p.m. (parts per million), respectively, in the vibrational–rotational lines. The hydrogen molecular ion is the only molecule for which theory and experiment have both been done accurately enough to require inclusion of these effects, as Professor Carrington's data demonstrate.

PHILOSOPHICAL TRANSACTIONS OF THE ROYAL SOCIETY A MATHEMATICAL, PHYSICAL & ENGINEERING SCIENCES